European Journal of Chemistry

Journal webpage: www.eurjchem.com

Design, synthesis and molecular docking studies of some morpholine linked thiazolidinone hybrid molecules

Javeed Ahmad War, Santosh Kumar Srivastava * and Savitri Devi Srivastava

Synthetic Organic Chemistry-Molecular Modelling Laboratory, Department of Chemistry, Dr. Hari Singh Gour University, Sagar, Madhya Pradesh, 470003, India

** Corresponding author at: Synthetic Organic Chemistry-Molecular Modelling Laboratory, Department of Chemistry, Dr. Hari Singh Gour University, Sagar, Madhya Pradesh, 470003, India.*
Tel.: +91.786.9351617. Fax: +91.786.9351617. E-mail address: profskssgr@gmail.com (S.K. Srivastava).

ARTICLE INFORMATION

DOI: 10.5155/eurjchem.7.3.271-279.1427

Received: 16 March 2016
Received in revised form: 10 April 2016
Accepted: 17 April 2016
Published online: 30 September 2016
Printed: 30 September 2016

KEYWORDS

Thiourea
Morpholine
Target fishing
Thiazolidinone
Molecular docking
Antimicrobial activity

ABSTRACT

A novel series of morpoline linked thiazolidione hybrid molecules targeting bacterial enoyl acyl carrier protein (Enoyl-ACP) reductase were designed and synthesized through a three step reaction protocol, which involves simple reaction setup and moderate reaction conditions. The synthesized molecules were characterized with FT-IR, ^{1}H NMR, ^{13}C NMR and HRMS techniques. *In vitro* susceptibility tests against some Gram positive (*Staphylococcus aureus* and *Bacillus subtilis*) and Gram negative bacteria (*Escherichia coli* and *Pseudomonas aeruginosa*) gave highly promising results. Most of the molecules were found to be active against the tested bacterial strains. The most potent molecule (S2B7) gave MIC value of 2.0 µg/mL against *Escherichia coli* that was better than the reference drug streptomycin. Structure activity relationship showed nitro and chloro groups are crucial for bioactivity if present at *meta* position of arylidene ring in designed molecules. Molecular docking simulations against multiple targets showed that the designed molecules have strong binding affinity towards Enoyl-ACP reductase. Binding affinity of -8.6 kcal/mol was predicted for S2B7. Van der Waals forces, hydrogen bonding and hydrophobic interactions were predicted as the main forces of interaction.

Cite this: *Eur. J. Chem.* **2016**, *7(3)*, 271-279

1. Introduction

With time, new classes of antimicrobial drugs were discovered and clinically used to treat patients with bacterial infections and related diseases [1]. In spite of initial success, they couldn't combat the emergence of multiple drug resistance (MDR). Over time microorganisms develop resistance to any drug, making them less effective [2-5]. Microorganisms have developed resistance to most of the current commercial antibiotics [6]. They develop resistance either by erroneous replication, modifying the drug target site or by exchange of resistant traits among themselves [7-9]. The global report of World Health Organization (WHO) on antimicrobial resistance (AMR) published in June, 2014 and updated in 2015 mentions that resistance of common bacteria to commercial antibiotics has reached alarming levels in many parts of the world. The report highlights that resistance to most widely used antibacterial medicines, fluoroquinolones and methicillin for the treatment of infections caused by *E. coli* and *S. aureus*, respectively, is very widespread [10]. This scenario poses a huge challenge of developing new classes of antibiotics which either have a different mechanism of action or possess high binding affinity towards the target site of resistant microbial strains. Any lack in development of new antimicrobial drugs is a serious threat to public health [11].

Morpholine moiety is of immense importance to medicinal chemists and has been used as core scaffold and capping fragment to design new drug molecules [12,13]. It forms functional unit in almost 19 FDA approved drugs [14]. One of the common drugs linezolid which belongs to the oxazolidinone class of antibiotics contains morpholine subunit. The main structural feature responsible for its popularity is the presence of oxygen atom, which is capable of participating in donor-acceptor type interactions with the substrate and thereby forms a strong complex with its target. Oxygen atom also complements the pharmacophoric performance by reducing the basicity of nitrogen. And finally, if morpholine subunit gets attached to a lipophillic scaffold it increases its bioavailability through oral administration by increasing aqueous solubility [15-18]. Likewise the chemistry of thiazolidine ring system is of considerable interest as it forms core structure of many biomolecules, commercial drugs [19]and synthetic molecules with promising antimicrobial, antifungal, anticancer and antidiabetic activity [20-28]. Combining multiple bioactive structural moieties into a single molecule usually complements the overall pharmacophoric performance and has been extensively used to design new

ISSN 2153-2249 (Print) / ISSN 2153-2257 (Online) © 2016 Atlanta Publishing House LLC - All rights reserved - Printed in the USA
http://dx.doi.org/10.5155/eurjchem.7.3.271-279.1427

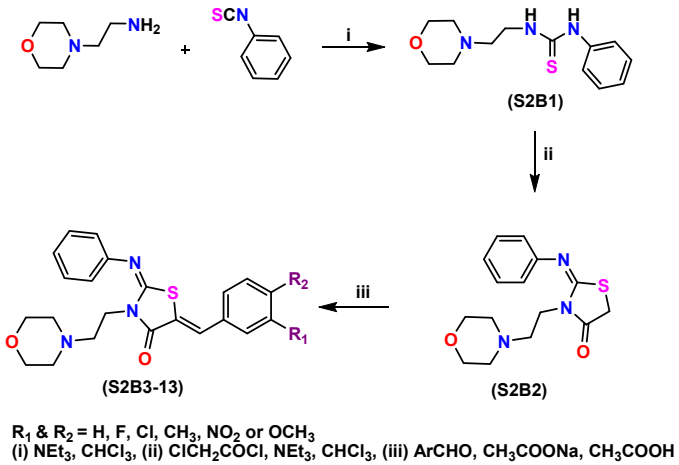

Figure 1. Reaction scheme for the synthesis of designed molecules.

drug candidates in structure based drug design [29,30]. Continuing our effort to build novel biologically active molecules [31,32] here, we designed morpholine linked thiazolidinone hybrid molecules with the aim of developing a new class of antimicrobials. The molecules were synthesized through a three step reaction protocol which involves simple reaction setup and moderate reaction conditions. *In vitro* susceptibility tests were carried against some selected Gram positive (*Staphylococcus aureus*, *Bacillus subtilis*) and Gram negative bacteria (*Escherichia coli* and *Pseudomonas aeruginosa*). *In silico* tools are continuously been used to design molecules with desired properties. Molinspiration and Orisis programs were used to calculate some crucial properties for the designed molecules. To our delight, the designed molecules gave excellent results for all such properties confirming the potential of such molecules as possible drugs.

When antibiotics act on particular bacteria, they either kill them (bactericidal) or stop their growth (bacterostatic). They do so by binding at cellular targets and inhibiting their normal function. The common targets being peptidoglycons in cell wall synthesis, plasma membrane, ribosomes in protein synthesis, translation, transcription, DNA/RNA replication pathway and metabolites of cell [33,34]. To predict the possible target for the designed molecules, molecular docking simulations were done against nine well established targets viz.; 1BNA, 1JZQ, 2RJG, 2VEG, 2ZDQ, 3TTZ, 3UDI, 1QG6 and 4URM. The top scored target was chosen as target for the synthesized molecules.

2. Experimental

2.1. Chemistry

Starting materials, reagents and solvents were purchased either from Merck or from Aldrich and were of reagent grade. Chemicals required for biological tests were purchased from HiMedia. Compounds were synthesized mostly under reflux conditions. Melting points were determined on an open capillary apparatus and are reported without correction. Infrared spectra were recorded on a Shimadzu FT-IR DR800 spectrophotometer with a resolution of 2 cm^{-1} in the range 400-4000 cm^{-1}. ^1H NMR spectra of compounds (in DMSO-d_6 or $CDCl_3$) were recorded on Bruker AV 500 spectrometer (Bruker, Karlsruhe, Germany) at 500 MHz. Peak multiplicities are designed as: s, singlet; d, doublet; dd, double doublet; t, triplet; td, triplet of doublets; m, multiplet. Chemical shifts (δ) are reported in ppm units relative to TMS as internal standard. High-resolution mass spectrometry was performed under ESI conditions at a resolution of 61800 using a Thermo Scientific Exactive mass spectrometer. Elemental analysis was done by Thermo Scientific FLASH-2000 CHN Analyzer. The values were within 0.4% of the calculated values. The reactions were monitored by TLC on $60F_{254}$ silica gel pre coated sheets (Merck, Darmstadt, Germany) which were visualized under UV (254 and 365 nm) light, with ethyl acetate: hexane (6:4, *v*:*v*) or chloroform: methanol (9:1, *v*:*v*) as solvent systems. The compounds were purified either by recrystallization or by column chromatography with 200-250 silica gel mesh.

2.2. Design

A careful survey of literature revealed the importance of morpholine and thiazolidinone moieties with respect to their biological potential. We therefore designed hybrid molecules with these moieties. Structural optimization of the final product with electron releasing (methyl, methoxy) and electron withdrawing functionality (nitro, halogens) was done with the aim of studying electronic effects on activity. Halogens, particularly fluorine and chlorine positively influence the biological properties of molecules. Halogen bonding has been found to be one of the factors by which chlorine alters the biological effect of molecules [35]. Substitution of hydrogen by fluorine usually has a positive impact on the activity of a molecule as fluorine is considered a classic bioisoster for hydrogen and methyl groups. And amongst halogens bromine has least prevalence in drugs so was left out while designing the molecules [36]. Taking these factors into consideration molecules were designed and later synthesized through a three step reaction protocol.

2.3. Synthesis

The designed compounds were synthesized by the multi-step reaction protocol (Figure 1). The first reaction (formation of thiourea) in the Figure 1 was carried out by reacting the appropriate amine with phenyl isothiocyanate in chloroform. After completion of the reaction, cyclisation of this intermediate was achieved by reacting it with chloroacetyl chloride in chloroform and catalytic amount of NEt_3. The final compounds (**S2B3-13**) in the series were obtained by refluxing the previous intermediates with commercially available aromatic aldehydes in presence of acetic acid and sodium acetate to facilitate the Knoevenagel condensation at the active methylene function of thiazolidinone ring.

2.3.1. General procedure for the synthesis of 1-(2-morpholinoethyl)-3-phenylthiourea (S2B1)

Phenyl isothiocyanate (15 g, 111.11 mmol) was dissolved in chloroform, and then 4-(2-aminoethyl)morpholine (8.11 g, 111.11 mmol) was added slowly at room temperature, and then refluxed for 8 hours, till white precipitate appeared. The precipitate was collected by filtration, washed with chloroform, and dried to afford product 1 as white powder. The product was recrystallized from ethanol (95%). The crystals were purified by column chromatography using chloroform:methanol (4:1, *v:v*) as eluent to afford the compound **S2B1** (Figure 1). Color: White. Yield: 90%. M.p.: 250-254 °C. FT-IR (KBr, ν, cm^{-1}): 3319, 3261 (NH, thiourea), 3055 (CH, aromatic). ^{1}H NMR (500 MHz, DMSO-d_6, δ, ppm): 2.39 (t, 4H, 1,5-CH_2), 3.37 (t, 4H, 2,4-CH_2), 3.56 (t, 2H, CH_2), 3.66 (t, 2H, CH_2), 7.10-7.40 (m, 5H, Ar-H), 7.60 (s, 1H, NH), 9.70 (s, 1H, NH). ^{13}C NMR (125 MHz, DMSO-d_6, δ, ppm): 179.79 (10CS), 137.06 (12C), 129.93 (14,16C), 126.88 (15C), 125.21 (13,17 C), 66.87 (2,4C), 55.68 (1,5C), 52.85 (7C), 41.02 (8C). HRMS (EI, *m/z*) calcd. for $C_{13}H_{19}N_3OS$, 265.12; found 265.25.

2.3.2. General procedure for the synthesis of (Z)-3-(2-morpholinoethyl)-2-(phenylimino)thiazolidin-4-one (S2B2)

To a solution of compound **S2B1** in chloroform, chloroacetyl chloride was added drop wise in presence of catalytic amount of NEt_3. The mixture was refluxed till the completion of reaction as monitored by TLC (18h). The solvent was evaporated. Removal of the solvent gives an oily residue, which was dissolved in diethyl ether and washed with an aqueous sodium carbonate (10%). The organic layer was dried over sodium sulphate, filtered, and concentrated (Figure 1). Color: Light brown. Yield: 72%. M.p.: 285-287 °C. FT-IR (KBr, ν, cm^{-1}): 1725 (C=O), 1635 (C=N), 1255 (NCS ring). ^{1}H NMR (500 MHz, DMSO-d_6, δ, ppm): 2.39 (t, 4H, N-CH_2-morpholine), 3.37 (t, 4H, O-CH_2-morpholine), 3.42 (t, 2H, CH_2), 3.56 (t, 2H, CH_2), 3.90 (2H, CH, thiazolidinone ring), 7.10-7.40 (m, 5H, Ar-H). ^{13}C NMR (125 MHz, DMSO-d_6, δ, ppm): 169.95 (10CO), 31.35 (11C), 152.52 (13C), 129.93 (17,19C), 126.88 (18C), 125.21 (16,20 C), 66.87 (2,4C), 55.68 (1,5C), 50.15 (7C), 44.12 (8C). HRMS (EI, *m/z*) calcd. for $C_{15}H_{19}N_3O_2S$, 305.12; found 305.36.

2.3.3. General procedure for the synthesis of (2Z,5E)-5-(substituted benzylidene)-3-(2-morpholinoethyl)-2-(phenylimino)thiazolidin-4-one (S2B3-13)

To a solution of compound **S2B2** (35 mmol) in acetic acid/sodium acetate buffer (50 mL), aromatic aldehydes (1.5 equiv.) were added in subsequent reactions to get the final products. The solution was refluxed till the completion of reaction as monitored by TLC. The reaction mixture was allowed to cool at room temperature, filtered and recrystallized from ethanol (Figure 1).

(2Z, 5E)-5-benzylidene-3-(2-morpholinoethyl)-2-(phenylimino)thiazolidin-4-one (**S2B3**): Color: Brown. Yield: 75%. M.p.: 390-395 °C. FT-IR (KBr, ν, cm^{-1}): 1710 (C=O), 1639 (C=N), 1250 (NCS ring). ^{1}H NMR (500 MHz, DMSO-d_6, δ, ppm): 2.39 (t, 4H, N-CH_2-morpholine), 3.12 (t, 2H, CH_2-N-Morpholine), 3.37 (t, 4H, O-CH_2-morpholine), 3.56 (t, 2H, CH_2-N-thiazolidinne), 6.90-7.40 (m, 11H, Ar-H + CH-arylidene). ^{13}C NMR (125 MHz, DMSO-d_6, δ, ppm): 167.35 (10CO), 117.21 (11C), 152.52 (13C), 129.93 (17,19C), 126.88 (18C), 125.21 (16,20 C), 66.87 (2,4 C), 55.68 (1,5 C), 52.85 (7C), 41.5 (8C), 142.25 (21C), 134.5 (22C), 128.5 (23,27C), 128.05 (24,26 C), 127.5 (25 C). HRMS (EI, *m/z*) calcd. for $C_{22}H_{23}N_3O_2S$, 393.15; found 393.45.

(2Z, 5E)-5-(3-fluorobenzylidene)-3-(2-morpholinoethyl)-2-(phenylimino)thiazolidin-4-one (**S2B4**): Color: Brown. Yield: 70 %. M.p.: 365-370 °C. FT-IR (KBr, ν, cm^{-1}): 1715 (C=O), 1070 (C-F). ^{1}H NMR (500 MHz, DMSO-d_6, δ, ppm): 2.39 (t, 4H, N-CH_2-morpholine), 3.12 (t, 2H, CH_2-N-Morpholine), 3.37 (t, 4H, O-CH_2-morpholine), 3.56 (t, 2H, CH_2-N-thiazolidinne), 6.80 (d, 1H, Ar-H), 7.01 (dd, 1H, *J* = 7.5 Hz, 3Hz, Ar-H), 7.09 (d, 1H, Ar-H), 7.10-7.40 (m, 7H, Ar-H + CH-arylidene). ^{13}C NMR (125 MHz, DMSO-d_6, δ, ppm): 167.35 (10CO), 117.21 (11C), 152.52 (13C), 129.93 (17,19 C), 126.88 (18C), 125.21 (16,20 C), 66.87 (2,4 C), 55.68 (1,5 C), 52.85 (7C), 41.5 (8C), 135.01 (21C), 117.05 (11C), 170.02 (10C), 150.3 (13C), 44.5 (8C), 134.5 (22C), 115.4 (23C), 164.5 (24C), 109.3 (25C), 125.5 (26C), 123.5 (27C). HRMS (EI, *m/z*) calcd. for $C_{22}H_{22}FN_3O_2S$, 411.14; found 411.18.

(2Z, 5E)-5-(3-chlorobenzylidene)-3-(2-morpholinoethyl)-2-(phenylimino)thiazolidin-4-one (**S2B5**): Color: Light brown. Yield: 70%. M.p.: 370-372 °C. FT-IR (KBr, ν, cm^{-1}): 1045 (C-Cl). ^{1}H NMR (500 MHz, DMSO-d_6, δ, ppm): 2.39 (t, 4H, N-CH_2-morpholine), 3.12 (t, 2H, CH_2-N-Morpholine), 3.37 (t, 4H, O-CH_2-morpholine), 3.56 (t, 2H, CH_2-N-thiazolidinne), 7.05 (s, 1H, CH-arylidene), 7.10-7.40 (m, 8H, Ar-H),7.53 (d, 1H, Ar-H). ^{13}C NMR (125 MHz, DMSO-d_6, δ, ppm): 167.35 (10CO), 117.21 (11C), 152.52 (13C), 129.93 (17,19 C), 126.88 (18C), 125.21 (16,20 C), 66.87 (2,4 C), 55.68 (1,5 C), 52.85 (7C), 41.5 (8C), 135.01 (21C), 117.05 (11C), 170.02 (10C), 150.3 (13C), 44.5 (8C), 134.6 (22C), 121.5 (23C), 133.5 (24C), 120.3 (25C), 126.01 (26C), 125.5 (27C). HRMS (EI, *m/z*) calcd. for $C_{22}H_{22}ClN_3O_2S$, 427.11; found 427.17.

(2Z, 5E)-5-(3-methylbenzylidene)-3-(2-morpholinoethyl)-2-(phenylimino)thiazolidin-4-one (**S2B6**): Color: Brown. Yield: 62%. M.p.: 362-365 °C. FT-IR (KBr, ν, cm^{-1}): 2955 (C-H). ^{1}H NMR (500 MHz, DMSO-d_6, δ, ppm): 2.31 (s, 3H, CH_3), 2.39 (t, 4H, N-CH_2-morpholine), 3.12 (t, 2H, CH_2-N-Morpholine), 3.37 (t, 4H, O-CH_2-morpholine), 3.56 (t, 2H, CH_2-N-thiazolidinne), 7.00 (s, 1H, CH- arylidene), 7.10-7.41 (m, 9H, Ar-H). ^{13}C NMR (125 MHz, DMSO-d_6, δ, ppm): 167.35 (10CO), 117.21 (11C), 152.52 (13C), 129.93 (17,19 C), 126.88 (18C), 125.21 (16,20 C), 66.87 (2,4 C), 55.68 (1,5C), 52.85 (7C), 41.5 (8C), 135.01 (21C), 117.05 (11C), 170.02 (10C), 150.3 (13C), 44.5 (8C), 134.5 (22C), 124.5 (23C), 136.5 (24C), 121.2 (25C), 124.3 (26C), 124.9 (27C). HRMS (EI, *m/z*) calcd. for $C_{23}H_{25}N_3O_2S$, 407.17; found 407.20.

(2Z, 5E)-3-(2-morpholinoethyl)-5-(3-nitrobenzylidene)-2-(phenylimino)thiazolidin-4-one (**S2B7**): Color: Yellow. Yield: 75 %. M.p.: 415-420 °C. FT-IR (KBr, ν, cm^{-1}): 1525 (N=O). ^{1}H NMR (500 MHz, DMSO-d_6, δ, ppm): 2.39 (t, 4H, N-CH_2-morpholine), 3.12 (t, 2H, CH_2-N-Morpholine), 3.37 (t, 4H, O-CH_2-morpho line), 3.56 (t, 2H, CH_2-N-thiazolidinne), 7.11-7.41 (m, 6H, Ar-H + CH-arylidene), 7.63 (td, 1H, Ar-H), 7.68 (dd, 1H, Ar-H), 8.15 (d, 1H, Ar-H), 8.32 (d, 1H, Ar-H). ^{13}C NMR (125 MHz, DMSO-d_6, δ, ppm): 167.35 (10CO), 117.21 (11C), 152.52 (13C), 129.93 (17,19 C), 126.88 (18C), 125.21(16,20 C), 66.87 (2,4 C), 55.68 (1,5 C), 52.85 (7C), 41.5 (8C), 135.01 (21C), 117.05 (11C), 170.02 (10C), 150.3 (13C), 44.5 (8C), 134.5 (22C), 119.5 (23C), 146.5 (24C), 120.01 (25C), 125.5 (26C), 134.5 (27C). HRMS (EI, *m/z*) calcd. for $C_{22}H_{22}N_4O_4S$, 438.14; found 438.35.

(2Z, 5E)-5-(3-methoxybenzylidene)-3-(2-morpholinoethyl)-2-(phenylimino)thiazolidin-4-one (**S2B8**): Color: Dark brown. Yield: 65 %. M.p.: 375-380 °C. FT-IR (KBr, ν, cm^{-1}): 1170 (C-O). ^{1}H NMR (500 MHz, DMSO-d_6, δ, ppm): 1.25 (s, 3H, OCH_3), 2.39 (t, 4H, N-CH_2-morpholine), 3.12 (t, 2H, CH_2-N-Morpholine), 3.37 (t, 4H, O-CH_2-morpholine), 3.56 (t, 2H, CH_2-N-thiazolidine), 7.05 (s, 1H, CH-arylidene), 7.10-7.41 (m, 8H, Ar-H), 7.53 (d, 1H, Ar-H). ^{13}C NMR (125 MHz, DMSO-d_6, δ, ppm): 167.35 (10CO), 117.21 (11C), 152.52 (13C), 129.93 (17,19 C), 126.88 (18C), 125.21 (16,20 C), 66.87 (2,4 C), 55.68 (1,5 C), 52.85 (7C), 41.5 (8C), 135.01 (21C), 117.05 (11C), 170.02 (10C), 150.3 (13C), 44.5 (8C), 134.5 (22C), 115.5 (23C), 162.2 (24C), 115.4 (25C), 125.4 (26C), 119.5 (27C). HRMS (EI, *m/z*) calcd. for $C_{23}H_{25}N_3O_3S$, 423.16; found 423.19.

(2Z, 5E)-5-(4-fluorobenzylidene)-3-(2-morpholinoethyl)-2-(phenylimino)thiazolidin-4-one (**S2B9**): Color: Brown. Yield: 65 %. M.p.: 385-390 °C. FT-IR (KBr, ν, cm^{-1}): 1155 (C-F). ^{1}H NMR (500 MHz, DMSO-d_6, δ, ppm): 2.39 (t, 4H, N-CH_2-morpholine), 3.12 (t, 2H, CH_2-N-Morpholine), 3.37 (t, 4H, O-CH_2-morpho line), 3.56 (t, 2H, CH_2-N-thiazolidinne), 7.11-7.39 (m, 8H, Ar-H

+ CH-arylidene), 7.55 (dd, 2H, Ar-H). ^{13}C NMR (125 MHz, DMSO-d_6, δ, ppm): 167.35 (10CO), 117.21 (11C), 152.52 (13C), 129.93 (17,19 C), 126.88 (18C), 125.21 (16,20 C), 66.87 (2,4 C), 55.68 (1,5C), 52.85 (7C), 41.5 (8C), 134.04 (21C), 116.07 (11C), 170.02 (10C), 150.3 (13C), 44.5 (8C), 131.5 (22C), 130.2 (23,27 C), 117.5 (24,26 C), 165.05 (25C). HRMS (EI, *m/z*) calcd. for $C_{22}H_{22}FN_3O_2S$, 411.14; found 411.17.

(2Z, 5E)-5-(4-chlorobenzylidene)-3-(2-morpholinoethyl)-2-(phenylimino)thiazolidin-4-one (**S2B10**): Color: Light brown. Yield: 72%. M.p.: 395-400 °C. FT-IR (KBr, ν, cm^{-1}): 1025 (C-Cl).^{1}H NMR (500 MHz, DMSO-d_6, δ, ppm): 2.39 (t, 4H, CH_2-morpholine), 3.12 (t, 2H, CH_2-N-Morpholine), 3.37 (t, 4H, O-CH_2-morpholine), 3.56 (t, 2H, CH_2-N-thiazolidinne), 7.10-7.42 (m, 10H, Ar-H + CH-arylidene). ^{13}C NMR (125 MHz, DMSO-d_6, δ, ppm): 167.35 (10CO), 117.21 (11C), 152.52 (13C), 129.93 (17,19 C), 126.88 (18C), 125.21 (16,20 C), 66.87 (2,4 C), 55.68 (1,5 C), 52.85 (7C), 41.5 (8C), 134.04 (21C), 116.07 (11C), 170.02 (10C), 150.3 (13C), 44.5 (8C), 132.5 (22C), 128.7 (23,27 C), 129.5 (24,26 C), 135.02 (25C). HRMS (EI, *m/z*) calcd. for $C_{22}H_{22}ClN_3O_2S$, 427.11; found 427.36.

(2Z, 5E)-5-(4-methylbenzylidene)-3-(2-morpholinoethyl)-2-(phenylimino)thiazolidin-4-one (**S2B11**): Color: Brown. Yield: 62 %. M.p.: 374-378 °C. FT-IR (KBr, ν, cm^{-1}): 2955 (C-H). ^{1}H NMR (500 MHz, DMSO-d_6, δ, ppm): 2.43 (s, 3H, CH_3), 2.39 (t, 4H, N-CH_2-morpholine), 3.12 (t, 2H, CH_2-N-Morpholine), 3.37 (t, 4H, O-CH_2-morpholine), 3.56 (t, 2H, CH_2-N-thiazolidinne), 7.11-7.41 (m, 8H, Ar-H + CH-arylidene), 7.52 (d, 2H, Ar-H). ^{13}C NMR (125 MHz, DMSO-d_6, δ, ppm): 167.35 (10CO), 117.21 (11C), 152.52 (13C), 129.93 (17,19 C), 126.88 (18C), 125.21 (16,20 C), 66.87 (2,4 C), 55.68 (1,5 C), 52.85 (7C), 41.5 (8C), 134.04 (21C), 116.07 (11C), 170.02 (10C), 150.3 (13C), 44.5 (8C), 131.2 (22C), 127.3 (23,27 C), 129.2 (24,26 C), 139.5 (25C). HRMS (EI, *m/z*) calcd. for $C_{23}H_{25}N_3O_2S$, 407.17; found 407.28.

(2Z, 5E)-3-(2-morpholinoethyl)-5-(4-nitrobenzylidene)-2-(phenylimino)thiazolidin-4-one (**S2B12**): Color: Yellow. Yield: 80 %. M.p.: 405-410 °C. FT-IR (KBr, ν, cm^{-1}): 1515 (C-NO_2). ^{1}H NMR (500 MHz, DMSO-d_6, δ, ppm): 2.39 (t, 4H, N-CH_2-morpho line), 3.12 (t, 2H, CH_2-N-Morpholine), 3.37 (t, 4H, O-CH_2-morpholine), 3.56 (t, 2H, CH_2-N-thiazolidinne), 7.10-7.41 (m, 6H, Ar-H + CH- arylidene), 7.69 (dd, 2H, Ar-H), 8.22 (d, 2H, Ar-H). ^{13}C NMR (125 MHz, DMSO-d_6, δ, ppm): 167.35 (10CO), 117.21 (11C), 152.52 (13C), 129.93 (17,19 C), 126.88 (18C), 125.21 (16,20 C), 66.87 (2,4 C), 55.68 (1,5 C), 52.85 (7C), 41.5 (8C), 134.04 (21C), 116.07 (11C), 170.02 (10C), 150.3 (13C), 44.5 (8C), 140.5 (22C), 129.2 (23,27 C), 126.5 (24,26 C), 147.5 (25C). HRMS (EI, *m/z*) calcd. for $C_{22}H_{22}N_4O_4S$, 438.14; found 438.35.

(2Z, 5E)-5-(4-methoxybenzylidene)-3-(2-morpholinoethyl)-2-(phenylimino)thiazolidin-4-one (**S2B13**): Color: Dark brown. Yield: 62 %. M.p.: 410-414 °C. FT-IR (KBr, ν, cm^{-1}): 1165 (C-O). ^{1}H NMR (500 MHz, DMSO-d_6, δ, ppm): 2.39 (t, 4H, N-CH_2-morpholine), 3.12 (t, 2H, CH_2-N-Morpholine), 3.37 (t, 4H, O-CH_2-morpholine), 3.56 (t, 2H, CH_2-N-thiazolidinne), 3.78 (s, 3H, OCH_3), 7.00 (d, 2H, Ar-H), 7.12-7.41 (m, 6H, Ar-H + CH-arylidene), 7.50 (dd, 2H, Ar-H). ^{13}C NMR (125 MHz, DMSO-d_6, δ, ppm): 167.35 (10CO), 117.21 (11C), 152.52 (13C), 129.93 (17,19 C), 126.88 (18C), 125.21 (16,20 C), 66.87 (2,4 C), 55.68 (1,5 C), 52.85 (7C), 41.5 (8C), 134.04 (21C), 116.07 (11C), 170.02 (10C), 150.3 (13C), 44.5 (8C), 126.3 (22C), 128.5 (27C), 112.16 (26C), 162.5 (25C). HRMS (EI, *m/z*) calcd. for $C_{23}H_{25}N_3O_3S$, 423.16; found 423.19.

2.4. Antimicrobial activity

Disk diffusion susceptibility method [37] in accordance with National Committee for Clinical Laboratory Standards (NCCLS) guidelines was used for initial screening of compounds for antibacterial activity against Gram positive (*B. subtilis* (MTCC10619) and *S. aureus* (MTCC 96)) and Gram negative bacteria (*P. aeruginosa* (MTCC1748) and *E. coli* (MTCC 68)). Pure microbial strains were obtained from MTCC IMTECH, Chandigarh, India. Müeller-Hinton agar (HiMedia) was melted and subsequently poured (20 mL) into Petri plates (100mm) and kept undisturbed at room temperature to solidify. A representative sample of the media was kept at 37 °C in BOD incubator for 24 hours to check the sterility. The culture of each bacterium in saline was uniformly spread over the media with a cotton swab. Sterile filter paper discs of 6 mm diameter (HiMedia) impregnated with particular concentration of compounds (in DMSO) was applied to the surface of inoculated plates. The plates were kept in BOD incubator for 24 hr at 37 °C and subsequently examined for bacterial growth. The results are expressed aszone of inhibition in millimeters (mm). Experiments were done in triplicate and on average standard deviation of < 2 were observed.

Agar dilution method [38] was used to calculate the MIC (minimum inhibitory concentration) of synthesized compounds. The pure bacterial strains were streaked onto nutrient rich (Mueller Hinton) agar plates to obtain single colonies. The plates were incubated at 37 °C for 22 hours. For each strain, four morphologically similar colonies were selected and transferred with a cotton swab into sterile capped glass tube containing sterile saline solution. Inoculum size for each test strain was adjusted to 104 CFU/mL (Colony Forming Unit per milliliter) with sterile saline through turbidimetric method. Stock solution of 1000 µg/mL for each compound was prepared in 1% DMSO. The stock solutions were further diluted with saline to get solutions of concentrations 500 to 2.4 µg/mL. 1mL each of the test solution and bacterial inoculum (104 CFU/mL) was mixed with nutrient agar and poured in petriplates. The plates were incubated at 37 °C for 24 hrs. MICs were defined as the lowest concentration of tested compound which prevented the visible growth of bacteria.

2.5. Molecular docking

Molecular docking calculations were performed on Autodock VINA software [39]. High resolution crystal structure of nine targets were downloaded from RCSB PDB website. The protein was prepared for docking by removing waters, co-factors (except NADH) and co-crystallized ligands using Discovery Studio Visualizer (DSV) 4.0. NADH was retained as the antimicrobial drugs acts complex with NADH. Atomic charges were calculated using Kollman method, polar hydrogens were added and finally grid dimensions (40×40×40 Å) were defined so as to include all the residues of the active site in Auto dock tools (ADT). For docking, the ligands were prepared by converting the 2D to 3D geometry followed by optimization at semi-empirical (PM3) level of theory. Atomic charges were calculated by Geistenger method. Torsions and rotatable bonds were defined in ADT. To test the accuracy of the docking protocol, the co-crystallized molecule (triclosan) was removed from the protein structure and was docked at the active site (to remove any crystallographic bias the ligand was drawn and optimized *de novo*). The docking protocol we employed predicted the same conformation as that in the crystal structure with RMSD values well within 1 Å (Figure 2). Autodock VINA predicts bound conformations and calculates the binding affinity. Both the parameters have significance while carrying virtual screening. Out of the nine conformations predicted by Autodock VINA for each molecule, the conformation which was close to co-crystallized ligand and scored well was chosen as the active conformation. These conformations were visualized in DSV (*Accelrys Software Inc.*) and LigandPlus [40] software to get insights into the interactions involved.

3. Results and discussions

3.1. Spectral analysis

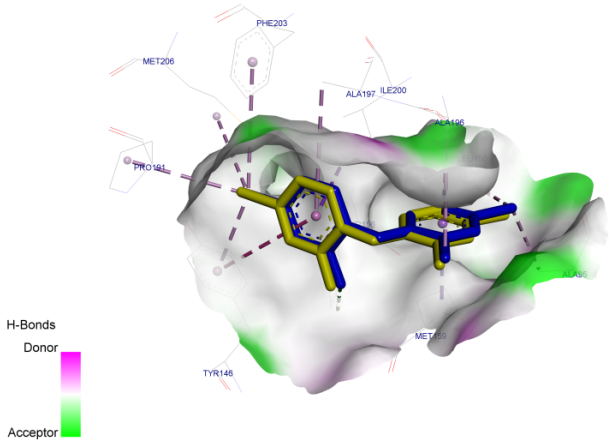

Figure 2. Superimposition of docked conformation (yellow) over the co-crystallized conformation(blue) of triclosan shows RMSD value close to zero, confirming the reliability of docking protocol. H-bonding surface and active site residues are shown for clarity.

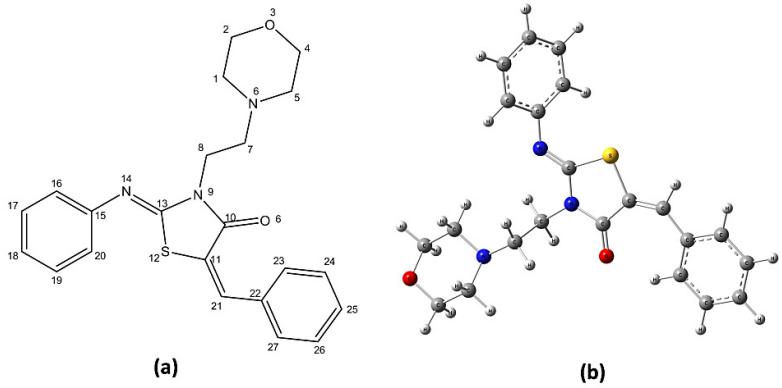

Figure 3. (a) Structure of **S2B3** with atom numbering for NMR interpretation, (b) DFT-B3LYP/6-31G(d,p) optimized geometry of **S2B3**.

The formation of compound **S2B1** (Figure 1) was confirmed by recording its FT-IR, ^{1}H NMR, ^{13}C NMR and HRMS spectra. Presence of N-H stretching vibrations at 3319 and 3261 cm^{-1} confirms the formation of thiourea. Shifts in aromatic C-H stretch (3055 cm^{-1}) and disappearance of primary amine vibrations corroborated the above results. ^{1}HNMR spectra of compound **S2B1** showed two broad singlets which were interpreted for thiourea N-H at δ 7.6 and 9.7 ppm. The most prominent peaks in ^{13}C NMR spectra at δ 179 ppm confirmed the presence of C=S linkage. The molecular ion peak ([M]$^{+}$ = 265.25 *m/z*) corresponded to the molecular mass of the compound.

The formation of compound **S2B2** was similarly confirmed from the corresponding spectra. FT-IR spectra show a sharp band at 1725 cm^{-1}, which was assigned for carbonyl C=O stretch. Disappearance of N-H and C=S stretching vibrations and presence of N=C and ring N-C-S vibrations at 1635 and 1255 cm^{-1} confirm the formation of thiazolidinone ring. ^{13}C NMR spectra shows peaks for carbonyl and methylene carbons at δ 169 and 31 ppm, respectively, which is consistent with formation of thiazolidinone ring. The molecular ion peak ([M]$^{+}$ = 305.36 *m/z*) corresponds to the molecular mass of the compound.

The final compounds **S2B3-13** were similarly characterized by recording the FT-IR, ^{1}H NMR and ^{13}C NMR spectra of the compounds. The absorption band at 1515 cm^{-1} in FT-IR spectra corresponds to arylidene C=C stretch. A singlet at δ 6.9-7.2 ppm and a multiplet at δ 6.9-8.1 ppm corresponding to CH and aromatic protons, respectively, confirmed the formation of the subsequent compounds. The substitution pattern in the phenyl ring was confirmed from the splitting pattern and corresponding coupling constants in the aromatic region of NMR spectra. A representative figure for **S2B3** with numbering for NMR interpretation is shown in Figure 3.

3.2. In silico study of drug likeness and molecular properties

As a starting point to evaluate the pharmaceutical potential of the synthesized molecules, we decided to calculate some *in silico* properties for these molecules. Most of the clinical drugs available in market possess some peculiar properties and it has been possible to quantitatively differentiate such properties (descriptors). A drug candidate should have certain structural features which increase its bioavailability and help it cross the blood brain barrier. It has become possible to quantify such structural features in terms of molecular properties like "Rule of five", Molecular Polar Surface Area (TPSA), Molecular Volume, Number of Rotatable Bonds (nrotb) *etc*. The Lipinski "Rule of five" [41] highlights the importance of physical parameters like lipophilicity (log P ≤ 5), molecular weight (≤ 500) and the number of hydrogen bond donors (≤ 10)/acceptors (≤ 10) for bioavailability and oral absorption. TPSA descriptor characterizes drug absorption, intestinal absorption, bioavailability, Caco-2 permeability and blood-brain barrier penetration [42].

Table 1. Orisis prediction of molecular volume, molecular total polar surface area (TPSA), drug score, number of rotatable bonds (nrotb) and solubility (log S).

Compound	Volume	Total polar surface area (TPSA)	Drug score	Number of rotatable bonds (nrotb)	log S, log (moles/L)
S2B3	356.92	46.84	0.34	5	-4.57
S2B4	361.85	46.84	0.43	5	-4.88
S2B5	370.46	46.84	0.50	5	-5.46
S2B6	373.48	46.84	0.39	5	-4.89
S2B7	380.25	92.67	-0.06	6	-5.34
S2B8	382.47	56.08	0.46	6	-4.71
S2B9	361.85	46.84	0.68	5	-5.09
S2B10	370.46	46.84	0.83	5	-5.53
S2B11	373.48	46.84	0.37	5	-5.03
S2B12	380.25	92.67	-0.11	6	-5.42
S2B13	382.47	56.08	0.50	6	-4.83

Table 2. Prediction of Lipinski parameters; *mi Log P* (Molinspiration Partitian Function), natoms (total no of atoms), MW (molecular weight), nON (no of hydrogen bond acceptors), nOHNH (no of hydrogen bond donors).

Compound	*mi Log P*	natoms	MW	nON	nOHNH	nviolations
S2B3	3.71	28	393.51	5	0	0
S2B4	3.98	23.0	411.50	5	0	0
S2B5	4.42	23.0	427.96	5	0	0
S2B6	4.11	23.0	407.54	5	0	0
S2B7	3.38	25.0	438.51	8	0	0
S2B8	3.80	24.0	423.54	6	0	0
S2B9	3.98	23.0	411.50	5	0	0
S2B10	4.42	23.0	427.96	5	0	0
S2B11	4.11	23.0	407.54	5	0	0
S2B12	3.38	25.0	438.51	8	0	0
S2B13	3.80	24.0	423.54	6	0	0

Table 3. MIC values in µg/mL±SD (n = 3) for the synthesized molecules calculated by agar dilution method (The experiments were done in triplicate).

Compound	Minimum inhibitory concentration (MIC) against bacteria in µg/mL ±SD			
	S. aureus (MTCC 96)	*B. subtilis* (MTCC 10619)	*E. coli* (MTCC 68)	*P. aeruginosa* (MTCC 1748)
S2B3	12.5±0.2	12.5±0.6	25±0.62	50±0.62
S2B4	12.5±0.1	6.25±0.9	3.125±0.60	12.5±0.2
S2B5	6.25±0.62	12.5±0.2	25±0.62	3.125±0.60
S2B6	25±0.62	50±0.62	12.5±0.2	200±0.62
S2B7	3.125±0.25	12.5±0.30	2.0±0.12	12.5±0.2
S2B8	6.25±0.62	12.5±0.0	50±0.62	25±1.62
S2B9	12.5±0.5	25±0.60	25±0.62	100±0.62
S2B10	6.25±0.62	25±0.62	50±0.62	12.5±0.6
S2B11	12.5±0.20	50±0.60	6.125±0.60	25±0.62
S2B12	12.5±0.5	50±0.30	12.5±0.2	6.25±0.60
S2B13	25±0.5	12.5±0.2	6.25±0.62	12.5±0.2
Ciprofloxacin	3.125±0.82	6.25±0.24	3.125±0.4	3.125±0.42
Streptomycin	6.25±0.62	3.125±0.2	6.25±0.6	3.125±0.42

Nrotb topological parameter is a measure of molecular flexibility and is a good descriptor for oral bioavailability [43]. Molecular properties for the synthesized compounds were calculated by Molinspiration and Orisis web servers are shown in Table 1 [44].

None of the synthesized molecules violates the Lipinski Rule of five. Among the synthesized compounds Orisis property explorer predicts the floro, chloro and methoxy derivatives to be better drug candidates in terms of oral absorption and overall bioavailability as compared to others however on an overall basis all the synthesized molecules score pretty well for all the calculated properties (Table 2). Halogens particularly fluorine and chlorine positively influence the biological properties of molecules. Halogen bonding has been found to be one of the factors by which chlorine alters the biological effect of molecules. The molinspiration predicts that the nitro derivatives because of large polar surface area show better interaction compared to other derivatives. From these studies it was found that the molecules possess drug like properties and can interact with biomolecules to exert a particular effect. Having satisfied ourselves with primary *in silico* screening assay of these compounds we decided to carry *in vitro* antimicrobial activity of these compounds to further investigate their biological potential.

3.3. Antimicrobial activity

As is evident from Table 3, compound **S2B7** was found to be the most active molecule in terms of MIC. MIC value of 2 µg/mL was found against *E. coli.* A look at the structure of **S2B7** shows that the structural feature responsible for its high activity is the presence of nitro group at the *meta* position wherein nitrogen and oxygen atoms provide polar surfaces for interaction with substrate molecules. A careful observation of MIC values shows that methyl substitution suppresses activity and presence of NO_2 and Cl groups enhance activity. As is evident from Table 3, most of the compounds inhibit the growth of both gram positive as well as Gram negative bacterial strains to substantial levels. Examining the MIC values (Table 3) shows **S2B7** to be most potent molecule against *P. aeruginosa* with MIC value 2.5 µg/mL which is better than the standard drugs Streptomycin and Ciprofloxacin with MIC value 3.125 µg/mL, this is followed by **S2B4** and **S2B11** with MIC value 3.125 and 6.25 µg/mL, respectively. The high activity of **S2B5** and **S2B12** against *P. aeruginosa* is attributed to the presence of Cl and NO_2 groups which both complement the activity. As reveled by docking these groups help the molecule to attain a conformation which fits the target site and binds through multiple interactions. For most of the compounds the docking scores how a good correlation with the MICs for compounds against *E. coli.* The most noticeable exception being **S2B11**. Upon examination of structure activity relationships it was observed that amongst the *para*-substituted derivatives *para*-nitro was found to be most potent. This may be due to the ability of NO_2 group to take part in donor-acceptorinteractions. Halogens in general and chlorine in particular increase the oral absorption and potency of a drug candidate [45]. Thus in addition to the bioactivity *para*-chloro derivatives might show good oral absorption as well. Further structural optimization might lead to more actives.

Table 4. Docking scores for docking of **S2B3** against different targets.

PDB ID	1BNA	1JZQ	2RJG	2VEG	2ZDQ	3TTZ	3UDI	1QG6	4URM
Docking Score (Kcal/mol)	-7.3	-8.3	-6.5	-6.6	-6.7	-6.4	-7.3	-8.6	-6.8

Table 5. Structures of the synthesized compounds with binding affinity values and the hydrogen bonding residues at the active site as predicted by AutoDock VINA.

Compound			Binding affinity (kcal/mol)	No of H-bonds	H-bonding residues
No	R_1	R_2			
S2B3	H	H	-8.6	01	Ile20
S2B4	F	H	-8.8	03	Ile20, Ile192, Gly93
S2B5	Cl	H	-8.6	02	Ile20
S2B6	CH_3	H	-8.7	01	Ile20
S2B7	NO_2	H	-8.6	01	Ile20
S2B8	OCH_3	H	-8.4	01	Ile20
S2B9	H	F	-8.5	01	Gly199
S2B10	H	Cl	-8.0	01	Gly93
S2B11	H	CH_3	-9.5	01	Thr194
S2B12	H	NO_2	-8.0	02	Thr194, Gly93, Tyr146 (π- π)
S2B13	H	OCH_3	-8.4	0	-

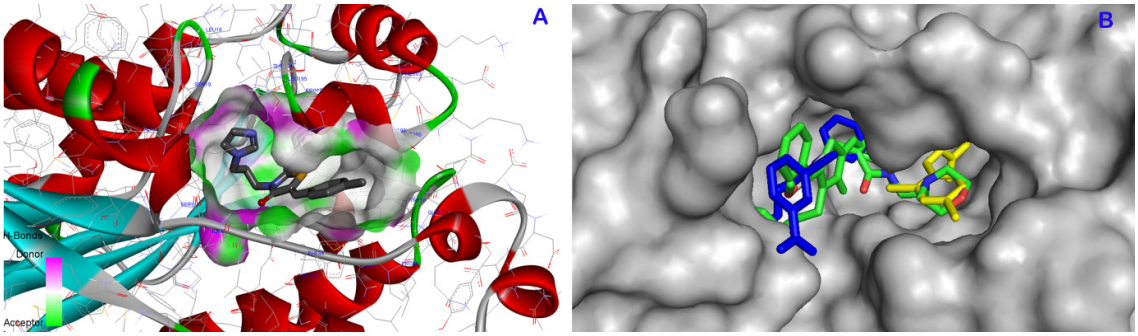

Figure 4. (a) Schematic representation for the docked conformation of the **S2B3** at the active site of Enoyl-ACP reductase with hydrophobic surface, (b) Surface representation of the protein showing the active site cavity. The docked ligand binds at the same site where co-crystallized Triclosan binds.

3.4. Molecular docking

The aim of carrying docking study was to first predict the molecular target for the synthesized molecules and later rationalize the experimental activity. The tested molecule **S2B3** was docked against nine different targets with PDB IDs; 1BNA, 1JZQ, 2RJG, 2VEG, 2ZDQ, 3TTZ, 3UDI, 1QG6 and 4URM [46-54]. As is evident from Table 4, the docking simulations predict that compound **S2B3** has the strongest binding affinity towards 1QG6. Based on the docking score Enoyl-ACP reductase was chosen as possible target and subsequently docking of all synthesized molecules was carried against this particular target.

Enoyl-ACP reductase is a key enzyme for fatty acid biosynthesis in bacteria. The biosynthetic pathway for fatty acid synthesis in bacteria is pretty different from that of mammals. This is of great advantage in designing molecules which are highly specific towards bacteria [55]. Molecular level understanding of the extent to which the molecules could inhibit the functioning of target macromolecule was studied by looking at the interactions involved between the target and inhibitor.

Trichlosan (co-crystallized with Enoyl-ACP reductase) is an antimicrobial drug which is ineffective against resistant strains of *E. coli* because amino acids Gly93, Met159 and Phe203 are mutated to Val, Thr and leu, respectively, at the active site. Therefore, for a drug to be active against the resistant strains of bacteria, they should be able to interact with the mutated as well as the non-mutated residues. From docking studies it is clear that the designed inhibitors bind at the same site where triclosan binds (Figure 4) and interact strongly with residues apart from the mutated ones (Figure 5). Binding affinity values ranging from -8.0 to -9.5 were predicted for the designed molecules (Table 5). The prominent interactions include H-bonding, alkyl-π and π-π stacking interactions. Most of the inhibitors interact with Ile20, Gly93 and NAD by forming strong hydrogen bonds. The formation of more than two H-bonds confers specificity to the inhibitors for the target. The highest binding affinity is predicted for **S2B11** followed by **S2B4**, **S2B6** and **S2B7**, respectively. Compound **S2B4** forms H-bonds with Ile20, Ile192 and Gly93. For compound **S2B12**, Thr194 and Gly93 form H-bonds whereas Tyr146 gets involved in a strong π-π stacking interaction. In conclusion docking simulations predict strong inhibitor-substrate interaction which is a highly desirable feature for drug candidates.

4. Conclusions

In conclusion, we were successful in establishing the initial hypothesis of synthesizing a novel class of hybrid molecules with broad spectrum antibiotic activity. As a starting point, *in silico* molecular descriptor calculations predicted drug like properties in the synthesized molecules, which were later confirmed by *in vitro* susceptibility tests against some Gram positive and negative bacteria. Molecular docking studies predicted the molecules as Enoyl-ACP reductase inhibitors. The compounds bind at the target site and get involved in Van der Waals, H-bonding and hydrophobic interactions. High binding affinity (-8.4 to -9.5 kcal/mol) was predicted for the inhibitors. Presence of nitro and chloro groups substantially increased the activity of molecules when present at *meta*/*para* position in the substituted phenyl ring. In conclusion the compounds we report have shown great promise for their antimicrobial potential. Further structural optimization may lead to discovery of other leads for antimicrobial drug discovery.

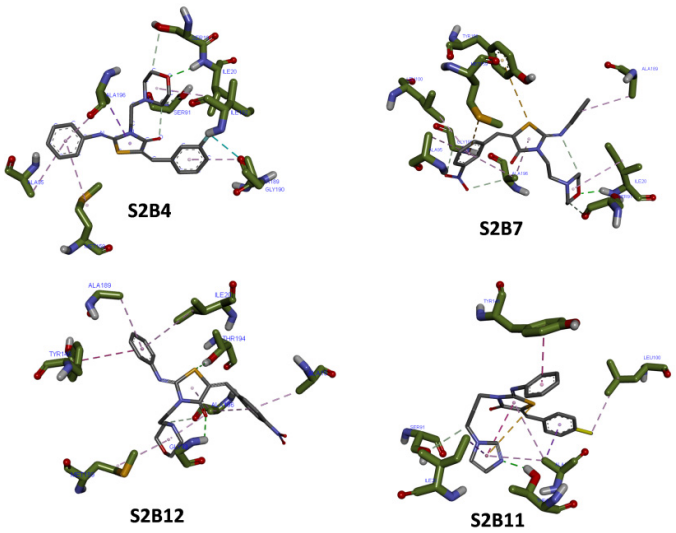

Figure 5. Detailed interactions of **S2B4**,**7**, **11** and **12** with the inhibitor residues, dotted lines represent the interactions. H bonds, π-π and alkyl-π interactions are represented by green, pink and violet dotted lines, respectively.

Acknowledgement

The authors would like to acknowledge Sophisticated Analytical Instrumental Facility (Panjab University, Chandigarh), Central Instrumentation Facility (Dr. Hari Singh Gour University, Sagar) and National Institute of Information Science and Technology (Kerala), India for providing instrument facility. Javeed Ahmad War acknowledges financial support from Department of Science and Technology, New-Delhi, India under INSPIRE program (INSPIRE ID: IF120399). Assistance of Mr. Arun Kumar (Department of Zoology, Dr. Hari Singh Gour University, Sagar) in carrying biological tests is highly acknowledged.

References

[1]. Scheffler, R.; Colmer, S.; Tynan, H.; Demain, A.; Gullo, V. *Appl. Microbiol. Biotechnol.* **2013**, *97*, 969-978.
[2]. Boucher, H. W.; Talbot, G. H.; Bradley, J. S.; Edwards, J. E.; Gilbert, D.; Rice, L. B.; Scheld, M.; Spellberg, B.; Bartlett, J. *Clin. Infect. Dis.* **2009**, *48*, 1-12.
[3]. Brandt, C.; Makarewicz, O.; Fischer, T.; Stein, C.; Pfeifer, Y.; Werner, G.; Pletz, M. W. *Int. J. Antimicrob. Agents* **2014**, *44*, 424-430.
[4]. Cohen, M. L. *Science* **1992**, *257*, 1050-1055.
[5]. Gagliotti, C.; Balode, A.; Baquero, F.; Degener, J.; Grundmann, H.; Gür, D.; Jarlier, V.; Kahlmeter, G.; Monen, J.; Monnet, D. *Euro. Surveill.* **2011**, *16(11)*, 1-5.
[6]. Tanwar, J.; Das, S.; Fatima, Z.; Hameed, S. *Interdiscip Perspect Infect Dis.* **2014**, *2014*, ID: 541340, 1-7.
[7]. Woolhouse, M. E.; Ward, M. J. *Science* **2013**, *341*, 1460-1461.
[8]. Lowy, F. D. *J. Clin. Invest.* **2003**, *111*, 1265-1273.
[9]. Rice, L. B. *Am. J. Infect. Control* **2006**, *34*, S11-S19.
[10]. Organization, W. H. World Health Organization, 2014.
[11]. Norrby, S. R.; Nord, C. E.; Finch, R. *Lancet Infect. Dis.* **2005**, *5*, 115-119.
[12]. Micheli, F.; Cremonesi, S.; Semeraro, T.; Tarsi, L.; Tomelleri, S.; Cavanni, P.; Oliosi, B.; Perdonà, E.; Sava, A.; Zonzini, L. *Bioorg. Med. Chem. Lett.* **2016**, *26*, 1329-1332.
[13]. Panneerselvam, P.; Nair, R. R.; Vijayalakshmi, G.; Subramanian, E. H.; Sridhar, S. K. *Eur. J. Med. Chem.* **2005**, *40*, 225-229.
[14]. Shcherbatiuk, A. V.; Shyshlyk, O. S.; Yarmoliuk, D. V.; Shishkin, O. V.; Shishkina, S. V.; Starova, V. S.; Zaporozhets, O. A.; Zozulya, S.; Moriev, R.; Kravchuk, O. *Tetrahedron* **2013**, *69*, 3796-3804.
[15]. Bissantz, C.; Kuhn, B.; Stahl, M. *J. Med. Chem.* **2010**, *53*, 5061-5084.
[16]. Morgenthaler, M.; Schweizer, E.; Hoffmann-Röder, A.; Benini, F.; Martin, R. E.; Jaeschke, G.; Wagner, B.; Fischer, H.; Bendels, S.; Zimmerli, D. *Chem. Med. Chem.* **2007**, *2*, 1100-1115.
[17]. Ndungu, J. M.; Krumm, S. A.; Yan, D.; Arrendale, R. F.; Reddy, G. P.; Evers, T.; Howard, R.; Natchus, M. G.; Saindane, M. T.; Liotta, D. C. *J. Med. Chem.* **2012**, *55*, 4220-4230.
[18]. Andrs, M.; Korabecny, J.; Jun, D.; Hodny, Z.; Bartek, J.; Kuca, K. *J. Med. Chem.* **2014**, *58*, 41-71.
[19]. Nazreen, S.; Alam, M. S.; Hamid, H.; Yar, M. S.; Shafi, S.; Dhulap, A.; Alam, P.; Pasha, M.; Bano, S.; Alam, M. M. *Eur. J. Med. Chem.* **2014**, *87*, 175-185.
[20]. Chavan, S.; Zangade, S.; Vibhute, A.; Vibhute, Y. *Eur. J. Chem.* **2013**, *4*, 98-101.
[21]. Devi, P. B.; Samala, G.; Sridevi, J. P.; Saxena, S.; Alvala, M.; Salina, E. G.; Sriram, D.; Yogeeswari, P. *Chem. Med. Chem.* **2014**, *9*, 2538-2547.
[22]. Hidalgo-Figueroa, S.; Ramírez-Espinosa, J. J.; Estrada-Soto, S.; Almanza-Pérez, J. C.; Román-Ramos, R.; Alarcón-Aguilar, F. J.; Hernández-Rosado, J. V.; Moreno-Díaz, H.; Díaz-Coutiño, D.; Navarrete-Vázquez, G. *Chem. Biol. Drug Des.* **2013**, *81*, 474-483.
[23]. Barros, F. W.; Silva, T. G.; da Rocha Pitta, M. G.; Bezerra, D. P.; Costa-Lotufo, L. V.; de Moraes, M. O.; Pessoa, C.; de Moura, M. A. F.; de Abreu, F. C.; de Lima, M. d. C. A. *Bioorgan. Med. Chem.* **2012**, *20*, 3533-3539.
[24]. Jain, A. K.; Vaidya, A.; Ravichandran, V.; Kashaw, S. K.; Agrawal, R. K. *Bioorgan. Med. Chem.* **2012**, *20*, 3378-3395.
[25]. Jain, V. S.; Vora, D. K.; Ramaa, C. *Bioorgan. Med. Chem.* **2013**, *21*, 1599-1620.
[26]. Keri, R. S.; Patil, M. R.; Patil, S. A.; Budagumpi, S. *Eur. J. Med. Chem.* **2015**, *89*, 207-251.
[27]. Shehab, W. S.; Mouneir, S. M. *Eur. J. Chem.* **2015**, *6*, 157-162.
[28]. Mushtaque, M.; Avecilla, F.; Azam, A. *Eur. J. Med. Chem.* **2012**, *55*, 439.
[29]. Welsch, M. E.; Snyder, S. A.; Stockwell, B. R. *Curr. Opin. Chem. Biol.* **2010**, *14*, 347-361.
[30]. Bansal, Y.; Silakari, O. *Eur. J. Med. Chem.* **2014**, *76*, 31-42.
[31]. Dubey, A.; Srivastava, S.; Srivastava, S. *Bioorg. Med. Chem. Lett.* **2011**, *21*, 569-573.
[32]. Upadhyay, A.; Srivastava, S.; Srivastava, S. *Eur. J. Med. Chem.* **2010**, *45*, 3541-3548.
[33]. Bürli, R. W.; Ge, Y.; White, S.; Baird, E. E.; Touami, S. M.; Taylor, M.; Kaizerman, J. A.; Moser, H. E. *Bioorg. Med. Chem. Lett.* **2002**, *12*, 2591-2594.
[34]. Kohanski, M. A.; Dwyer, D. J.; Collins, J. J. *Nat. Rev. Microbiol.* **2010**, *8*, 423-435.
[35]. Auffinger, P.; Hays, F. A.; Westhof, E.; Ho, P. S. *Proc. Natl. Acad. Sci. USA* **2004**, *101*, 16789-16794.
[36]. Hernandes, M. Z.; Cavalcanti, S. M. T.; Moreira, D. R. M.; de Azevedo, J.; Filgueira, W.; Leite, A. C. L. *Curr. Drug Targets* **2010**, *11*, 303-314.
[37]. Drew, W. L.; Barry, A.; O'Toole, R.; Sherris, J. C. *Appl. Microbiol.* **1972**, *24*, 240-247.
[38]. Wiegand, I.; Hilpert, K.; Hancock, R. E. *Nat. Protoc.* **2008**, *3*, 163-175.
[39]. Trott, O.; Olson, A. J. *J. Comput. Chem.* **2010**, *31*, 455-461.
[40]. Wallace, A. C.; Laskowski, R. A.; Thornton, J. M. *Protein Eng.* **1995**, *8*, 127-134.
[41]. Lipinski, C. A.; Lombardo, F.; Dominy, B. W.; Feeney, P. J. *Adv. Drug Deliver Rev.* **2012**, *64*, 4-17.
[42]. Ertl, P.; Rohde, B.; Selzer, P. *J. Med. Chem.* **2000**, *43*, 3714-3717.
[43]. Veber, D. F.; Johnson, S. R.; Cheng, H. Y.; Smith, B. R.; Ward, K. W.; Kopple, K. D. *J. Med. Chem.* **2002**, *45*, 2615-2623.
[44]. Sander, T.; Freyss, J.; von Korff, M.; Reich, J. R.; Rufener, C. *J. Chem. Inf. Model.* **2009**, *49*, 232-246.

[45]. Domagala, J. M. *J. Antimicrob. Chemother.* **1994**, *33*, 685-706.
[46]. Drew, H. R.; Wing, R. M.; Takano, T.; Broka, C.; Tanaka, S.; Itakura, K.; Dickerson, R. E. P *Natl. Acad. Sci. USA* **1981**, *78*, 2179-2183.
[47]. Levy, C.; Minnis, D.; Derrick, J. P. *Biochem. J.* **2008**, *412*, 379-388.
[48]. Lu, Y.; Liu, Y.; Xu, Z.; Li, H.; Liu, H.; Zhu, W. *Expert Opin. Drug Dis.* **2012**, *7*, 375-383.
[49]. Nakama, T.; Nureki, O. *J. Biol. Chem.* **2001**, *276*, 47387-47393.
[50]. Wu, D.; Hu, T.; Zhang, L.; Chen, J.; Du, J.; Ding, J.; Jiang, H.; Shen, X. *Protein Sci.* **2008**, *17*, 1066-1076.
[51]. Han, S.; Caspers, N.; Zaniewski, R. P.; Lacey, B. M.; Tomaras, A. P.; Feng, X.; Geoghegan, K. F. *J. Am. Chem. Soc.* **2011**, *133*, 20536-20545.
[52]. Lu, J.; Patel, S.; Sharma, N.; Soisson, S. M.; Kishii, R.; Takei, M.; Fukuda, Y.; Lumb, K. J.; Singh, S. B. *ACS Chem. Biol.* **2014**, *9*, 2023-2031.
[53]. Sherer, B. A.; Hull, K.; Green, O.; Basarab, G.; Hauck, S.; Hill, P.; Loch, J. T.; Mullen, G.; Bist, S.; Bryant, J.; Boriack-Sjodin, A.; Read, J.; DeGrace, N.; Uria-Nickelsen, M.; Illingworth, R. N.; Eakin, A. E. *Bioorg. Med. Chem. Lett.* **2011**, *21*, 7416-7420.
[54]. Ward, W. H.; Holdgate, G. A.; Rowsell, S.; McLean, E. G.; Pauptit, R. A.; Clayton, E.; Nichols, W. W.; Colls, J. G.; Minshull, C. A.; Jude, D. A.; Mistry, A.; Timms, D.; Camble, R.; Hales, N. J.; Britton, C. J.; Taylor, I. W. *Biochemistry-US* **1999**, *38*, 12514-12525.
[55]. McMurry, L. M.; Oethinger, M.; Levy, S. B. *Nature* **1998**, *394*, 531-532.